Inorg. Chem. **2004**, *43*, 7978–7985

Influence of the Halogen Ligand on the Near-UV–Visible Spectrum of [Ru(X)(Me)(CO)$_2$(α-diimine)] (X = Cl, I; α-Diimine = Me-DAB, iPr-DAB; DAB = 1,4-Diaza-1,3-butadiene): An ab Initio and TD-DFT Analysis

S. Záliš,*,† N. Ben Amor,‡ and C. Daniel*,‡

Laboratoire de Chimie Quantique UMR 7551 CNRS, Université Louis Pasteur Institut LeBel, 4 Rue Blaise Pascal, 67 000 Strasbourg, France, and J. Heyrovský Institute of Physical Chemistry, Academy of Sciences of the Czech Republic, Dolejškova 3, 182 23 Prague 8, Czech Republic

Received April 26, 2004

The near-UV–vis electronic spectroscopy of [Ru(X)(Me)(CO)$_2$(iPr-DAB)] (X = Cl or I; iPr-DAB = *N*,*N*′-di-isopropyl-1,4-diaza-1,3-butadiene) is investigated through CASSCF/CASPT2 and TD-DFT calculations on the model complexes [Ru(X)(Me)(CO)$_2$(Me-DAB)] (X = Cl or I). Convergence of the calculated transition energies for the low-lying metal-to-ligand charge-transfer (MLCT), X-to-ligand charge-transfer (XLCT, X halide ligand), or σ-bond-to-ligand charge-transfer (SBLCT) to experimental values is analyzed for both methods. On the basis of these accurate calculations, it is shown that whereas the lowest singlet state can be assigned to a nearly pure XLCT state in [Ru(I)(Me)(CO)$_2$(Me-DAB)], its character is mainly MLCT in [Ru(Cl)(Me)(CO)$_2$(Me-DAB)]. These results are in agreement with time-resolved emission/IR and resonance Raman experimental data. The experimental UV–vis bands are well reproduced by the CASSCF/CASPT2 calculations. The TD-DFT transition energies to the long-range charge transfer states are dramatically affected by the nature of the functional, with lowering leading to meaningless values in the case of nonhybrid functionals. Both methods reproduce well the red shift of the absorption bands on going from the chloride to the iodide complex as well as the shift of the strongly absorbing higher MLCT transition from the visible to the UV domain of energy.

Introduction

Transition metal carbonyl−diimine complexes [Re (X)-(CO)$_3$(α-diimine)] (X = halide, N-donor ligand; α-diimine = bpy, ^{i}Pr-PyCa, ^{i}Pr-DAB)[1−6] or [Ru(E)(E′)(CO)$_2$(α-diimine)] (E, E′ = halide, alkyl, benzyl, metal fragment; α-diimine = 1,4-diazabutadiene or 2,2′-bipyridine) are widely studied for their unconventional photochemical, photophysical, and electrochemical properties.[7−20] These molecules have great potential as luminophores, probes, photosensitizers, and photoinitiators of radical reactions and represent a challenge to the understanding of excited state dynamics.[21] The ruthenium complexes are particularly versatile, and their excited state properties may be varied out by independent replacement of the E and E′ ligands at either

* To whom correspondence should be addressed. E-mail: daniel@quantix.u-strasbg.fr.

† Academy of Sciences of the Czech Republic.

‡ Université Louis Pasteur Institut LeBel.

(1) Stufkens, D. J. *Comments Inorg. Chem.* **1992**, *13*, 359.
(2) Oriskovich, T. A.; White, P. S.; Thorp, H. H. *Inorg. Chem.* **1995**, *34*, 1629.
(3) Kotch, T. G.; Lees, A. J.; Fuerniss, S. J.; Papathomas, K. I.; Snyder, R. W. *Inorg. Chem.* **1993**, *32*, 2570.
(4) Thornton, N. B.; Schanze, K. S. *Inorg. Chem.* **1993**, *32*, 4994.
(5) Ishitani, O.; George, M. W.; Ibusuki, T.; Johnson, F. P. A.; Koike, K.; Nozaki, K.; Pac, S.; Turner, J. J.; Westwell, J. R. *Inorg. Chem.* **1994**, *33*, 4712.
(6) Grätzel, M. *Coord. Chem. Rev.* **1991**, *111*, 167.
(7) Nieuwenhuis, H. A.; Stufkens, D. J.; Oskam, A. *Inorg. Chem.* **1994**, *33*, 3212.
(8) Nieuwenhuis, H. A.; Stufkens, D. J.; Vlček, A., Jr. *Inorg. Chem.* **1995**, *34*, 3879.
(9) Nieuwenhuis, H. A.; Stufkens, D. J.; McNicholl, R. A.; Al-Obaidi, A. H. R.; Coates, C. G.; Bell, S. E. J.; McGarvey, J. J.; Westwell, J.; George, M. W.; Turner, J. J. *J. Am. Chem. Soc.* **1995**, *117*, 5579.
(10) Nieuwenhuis, H. A.; Van de Ven, M. C. E.; Stufkens, D. J.; Oskam, A.; Goubitz, K. *Organometallics* **1995**, *14*, 780.
(11) Aarnts, M. P.; Wilms, M. P.; Peelen, K.; Fraanje, J.; Goubitz, K.; Hartl, F.; Stufkens, D. J.; Baerends, E. J.; Vlček, A., Jr. *Inorg. Chem.* **1996**, *35*, 5468.
(12) Aarnts, M. P.; Stufkens, D. J.; Vlček, A., Jr. *Inorg. Chim. Acta* **1997**, *266*, 37.
(13) Aarnts, M. P.; Stufkens, D. J.; Oskam, A.; Fraanje, J.; Goubitz, K. *Inorg. Chim. Acta* **1997**, *256*, 93.
(14) Aarnts, M. P.; Hartl, F.; Peelen, K.; Stufkens, D. J.; Amatore, C.; Verpeaux, J. N. *Organometallics* **1997**, *16*, 4686.

10.1021/ic049464e CCC: $27.50
Published on Web 11/13/2004

of the two axial positions. In particular, the nature of the lowest excited state in [Ru(X)(R)(CO)$_2$(α-diimine)] (X = Cl or I; R = Me) may be tuned broadly from MLCT to XLCT long-lived excited states (MLCT stands for metal-to-ligand charge-transfer and XLCT for halide (X)-to-ligand charge-transfer), each of these excited states having its own properties and dynamics. As a general trend, it appears that both the emission lifetime and quantum yield decrease as a function of the emissive state character in the order XLCT > MLCT. Similarly, the photoreactivity of this class of molecules is dramatically influenced by the ligand R and the nature of the α-diimine group. For instance, the complexes [Ru(I)(R)(CO)$_2$(^{i}Pr-DAB)] (R = ^{i}Pr, Bzl) show a high efficiency for their homolysis reaction, whereas the methyl and ethyl complexes do not undergo such a reaction.[10]

On the basis of preliminary DFT calculations performed on the model system [Ru(Cl)(Me)(CO)$_2$(H-DAB)], the visible absorption bands observed for [Ru(Cl)(Me)(CO)$_2$(^{i}Pr-DAB)] have been assigned to a mixed metal/halide-to-DAB charge-transfer transition which corresponds mainly to d_{xz}(Ru)/p_z(Cl) → π^*_{DAB} excitation.[12−15,19] This transition is denoted as MLCT/XLCT. However, these early calculations did not reproduce the large red shift of the main visible absorption band observed on replacing the Cl ligand by $SnPh_3$ group, casting some doubt on the overall spectral assignment. Moreover, resonance Raman (rR) spectra of [Ru(X)(Me)(CO)$_2$(^{i}Pr-DAB) (X = Cl, I) show that the lowest-energy transition of the X = Cl complex affects both the imine and CO bonds (characteristic of MLCT transitions) whereas for X = I only the imine bonds are influenced by this transition (characteristic of charge transfer to the $\pi^*_{^iPr-DAB}$). From these experiments, as well as from time-resolved emission and IR spectroscopy, it has been concluded that the variation of halide from Cl to I gives rise to a change in character of the lowest energy band from MLCT to XLCT. [12−15]

In a recent work,[22] a detailed theoretical investigation of electronic transitions of the more realistic model complexes [Ru(E)(E′)(CO)$_2$(Me-DAB)] (E = E′ = SnH_3 or Cl; E = Me, E′ = SnH_3 or Cl) was undertaken, using different quantum chemical techniques, namely the CASSCF/CASPT2 and TD-DFT methods. On the basis of the calculated transition energies and oscillator strengths, it has been possible to assign without any ambiguity the UV−vis electronic spectra of the nonhalide complexes, namely [Ru($SnPh_3$)$_2$(CO)$_2$(^{i}Pr-DAB)] and [Ru($SnPh_3$)(Me)(CO)$_2$(^{i}Pr-DAB)], the agreement between the CASSCF/CASPT2 and TD-DFT approaches being remarkably good. In contrast, these two approaches lead to different descriptions of electronic transitions of the halide complexes [Ru(Cl)$_2$(CO)$_2$(^{i}Pr-DAB)] and [Ru(Cl)(Me)(CO)$_2$(^{i}Pr-DAB)]. The TD-DFT method systematically underestimated the transition energies; nevertheless, it reproduced the general spectral features. Whereas the CASSCF/CASPT2 method assigns the lowest-energy absorption to predominantly Ru → DAB MLCT transitions, TD-DFT predicts a mixed XLCT/MLCT character, with the XLCT component being predominant. Analysis of Kohn−Sham orbitals exhibits a very important $3p_{Cl}$ admixture into the high-lying occupied orbitals, in contrast to the CASSCF/CASPT2 molecular orbitals which are nearly pure $4d_{Ru}$ with the usual contribution of the back-donation to π_{CO} orbitals.

In a recent review article, the different methods of quantum chemistry were discussed within the context of the electronic spectroscopy and photoreactivity in transition metal complexes.[23] Their optical spectra have been interpreted by means of the DFT method, so-called Δ-SCF for a long time.[24] The TD-DFT is an alternative to this time-independent DFT method applied with success to highly symmetric molecules with several limitations.[25] The use of approximate exchange-correlation functionals with incorrect asymptotic behavior may lead to dramatic errors in the case of the TD-DFT method for two reasons:[26] (i) the most polarizable part of the charge density is at large *r*, and (ii) the asymptotic behavior of the exchange-correlation potential υ_{xc} determines the ionization threshold. The accuracy of the response calculation is very sensitive to the approximation made for υ_{xc} as well as to its repercussion on its derivative $\partial\upsilon_{xc}/\partial\rho$ (derivative discontinuity in the bulk region). Due to underestimation of the attractive character of the exchange-correlation potential, the charge density will be too diffuse. Consequently, the ionization threshold will be systematically too low with a dramatic effect on high excitation energies and polarizabilities which will be overestimated. Excitation involving a substantial change in the charge density distribution such as charge-transfer states will be described with difficulty by conventional functionals.[27] This failure of TD-DFT for long-range charge-transfer excited states is illustrated and analyzed in three recent papers.[28,29] Despite these drawbacks, the TD-DFT approach remains a computationally simple and efficient method able to treat practical problems in a reasonable time scale at a low cost when

(15) Aarnts, M. P.; Wilms, M. P.; Stufkens, D. J. *Organometallics* **1997**, *16*, 2055.
(16) Aarnts, M. P.; Oskam, A.; Stufkens, D. J.; Fraanje, J.; Goubitz, K.; Veldman, N.; Spek, A. L. *J. Organomet. Chem.* **1997**, *531*, 191.
(17) Stufkens, D. J.; Aarnts, M. P.; Nijhoff, J.; Rossenaar, B. D.; Vlček, A., Jr. *Coord. Chem. Rev.* **1998**, *171*, 93.
(18) Stufkens, D. J.; Vlček, A., Jr. *Coord. Chem. Rev.* **1998**, *177*, 27.
(19) Aarnts, M. P.; Stufkens, D. J.; Wilms, M. P.; Baerends, E. J.; Vlček, A., Jr.; Clark, I. P.; George, M. W.; Turner, J. J. *Chem.—Eur. J.* **1996**, *2*, 1556.
(20) Van Slageren, J.; Stufkens, D. J. *Inorg. Chem.* **2001**, *40*, 277.
(21) Turki, M.; Daniel, C. *Coord. Chem. Rev.* **2001**, *216−217*, 31.
(22) Turki, M.; Daniel, C.; Záliš, S.; Vlček A., Jr.; Van Slageren, J.; Stufkens, D. J. *J. Am. Chem. Soc.* **2001**, *123*, 11431.
(23) Daniel, C. *Coord. Chem. Rev.* **2003**, *238*, 143.
(24) Ziegler, T.; Rauk, A.; Baerends, E. J. *Theor. Chim. Acta* **1977**, *43*, 261. Daul, C. *Int. J. Quantum Chem., Quantum Chem. Symp.* **1994**, *52*, 867.
(25) Jamorski, C.; Casida, M. E.; Salahub, D. R. *J. Chem. Phys.* **1996**, *104*, 5134.
(26) Recent developments and applications of modern DFT. In *JMS Ed*; Casida, M. E., Ed.; Elsevier Science: Amsterdam, 1996; pp 391−434.
(27) Tozer, D. J.; Amos, R. D.; Handy, N. C.; Roos, B. O.; Serrano-Andres, L. *Mol. Phys.* **1999**, *97*, 859. Casida, M. E.; Gutierrez, F.; Guan, F.-X.; Gadea, D. R.; Salahub, J.-P.; Daudey, J. *Chem. Phys.* **2000**, *113*, 7062.
(28) Szilagyi, R. K.; Metz, M.; Solomon, E. I. *J. Phys. Chem. A* **2002**, *106*, 2994.
(29) Dreuw, A.; Head-Gordon, M. *J. Am. Chem. Soc.* **2004**, *126*, 4007. Gritsenko, O.; Baerends, E. J. *J. Chem. Phys.* **2004**, *121*, 655.

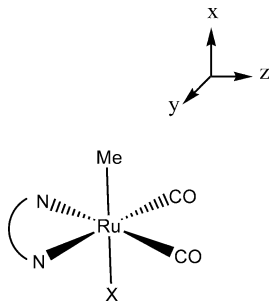

Figure 1. Idealized structure of the complexes $[Ru(X)(Me)(CO)_2(Me\text{-}DAB)]$ (X = Cl, I) and chosen orientation of the axis.

compared with highly correlated ab initio methods.[23] However, the expertise is not sufficient with respect to the ability of the functionals to describe a variety of excited states, and additional validation has to be performed in some perverse cases.

The purpose of the present study is 2-fold: (i) the investigation of the influence of the functionals on the TD-DFT transition energies and spectral assignment in $[Ru(E)(E')(CO)_2(\alpha\text{-diimine})]$ (E = Cl, E′ = Me and E = SnH_3, E′ = Me);[22] (ii) the study of the influence of the halide ligand on the absorption spectra in order to explain the observed differences in absorption/emission and photoreactivity when going from the chloride to the analogous iodide.[7] A comparison between the different quantum chemical methods (CASSCF/CASPT2, TD-DFT) and other computational details is discussed elsewhere.[30]

Structure and Bonding

The CASSCF/CASPT2 ab initio calculations have been performed on the DFT (B3LYP) optimized structures[31] of the electronic ground states in C_s symmetry for $[Ru(Cl)(Me)(CO)_2(Me\text{-}DAB)]$ and $[Ru(I)(Me)(CO)_2(Me\text{-}DAB)]$ (see Figure 1).

The $^1A'$ electronic ground-state configuration is given by the following formal molecular orbitals occupation: $(3p_z(Cl))^2(\sigma 1_{ClRuMe})^2(4d_{xy})^2(4d_{y^2-z^2})^2(\sigma 2_{ClRuMe})^2(4d_{xz})^2$ for $[Ru(Cl)(Me)(CO)_2(Me\text{-}DAB)]$ and $(4d_{y^2-z^2})^2(\sigma 1_{IRuMe})^2(4d_{xy})^2(4d_{xz}/5p_z(I))^2(\sigma 2_{IRuMe})^2(5p_z(I)/4d_{xz})^2$ for $[Ru(I)(Me)(CO)_2(Me\text{-}DAB]$. $\sigma 1_{ClRuMe}$ and $\sigma 1_{IRuMe}$ orbitals are bonding combinations of the $4d_{Ru}$ orbital of the metal center with the sp^3-like C of the methyl ligand and the sp(X) (X = Cl, I). $\sigma 2_{ClRuMe}$ and $\sigma 2_{IRuMe}$ are bonding combinations between the $5p_{Ru}$ orbital of the metal center and the sp^3-like C of the methyl ligand and $4d_{Ru}$/sp(X) (X = Cl, I) nonbonding (Scheme 1).

A careful analysis of the CASSCF MOs depicted in Scheme 1 points to significant differences between the chloride and the iodide complex already at the electronic ground-state structure level. In particular, the $4d_{xz}$ orbital is nearly pure in $[Ru(Cl)(Me)(CO)_2(Me\text{-}DAB)]$ whereas it is largely mixed with the $5p_x(I)$ in $[Ru(I)(Me)(CO)_2(Me\text{-}DAB)]$. This will have a profound consequence on the electronic

Scheme 1

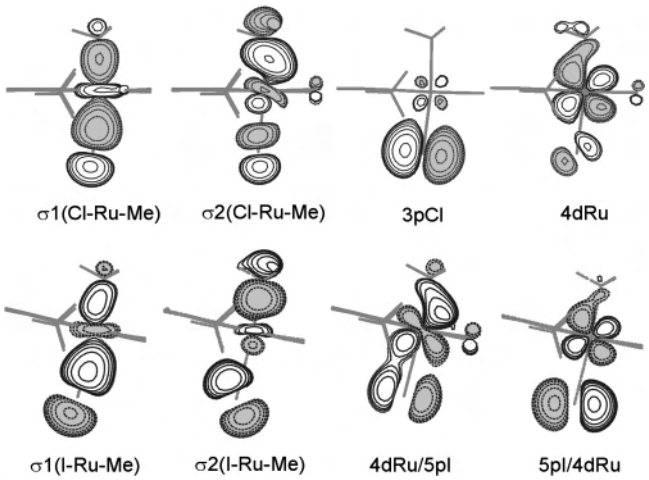

Scheme 2

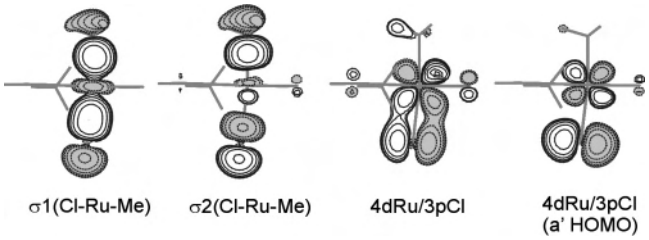

spectra of these molecules as will be illustrated by the results reported in the next sections.

Kohn−Sham (KS) orbitals for the chloride complex are presented in Scheme 2. In contrast to the CASSCF MOs, the $4d_{Ru}$ and 3p(Cl) KS orbitals are mixed leading to a bonding $4d_{Ru}$/3p(Cl) combination and to its 3p(Cl)/$4d_{Ru}$ antibonding counterpart. The KS orbitals of the iodide analogue do not differ substantially from those of the chloride complex described in Scheme 2: 4p(I)/$4d_{Ru}$ is more localized on I and $4d_{Ru}$/4p(I) on Ru than in the case of the Cl complex.

Computational Methods

Other details of the calculations are reported elsewhere (basis sets influence, CASSCF active space, etc.).[30] On the basis of this careful computational study, the best CASSCF wave functions with respect to the photophysics of the molecules have been used as references in subsequent CASPT2 calculations using the level shift corrected perturbation method.[32] There are 16 electrons correlated in 15 orbitals ($3p_z(X)$, $3p_y(X)$, $\pi_{DAB}/4d_{xy}$, $4d_{xy}$, $4d_{xz}$, $4d_{x^2-y^2}$, $\sigma 1_{XRuMe}$, $\sigma 2_{XRuMe}$, $\sigma 1^*_{XRuMe}$, $\sigma 2^*_{XRuMe}$, $4d'/\pi^*_{CO}(4)$) in this CASSCF calculation where the total energy is averaged over the six lowest roots. Relativistic effective core potentials have been used with the following associated valence basis sets: for the Ru atom (16 valence electrons), a (8s, 7p, 6d) set contracted to [6s, 5p, 3d],[33] for the second row atoms, C (4 valence electrons) a (4s, 4p) set contracted to [2s, 2p],[34] and O (6 valence electrons) a (4s, 5p) set contracted [2s, 3p].[34] For the chloride atom (7 valence electrons) a (4s, 5p)

(30) Ben Amor, N.; Daniel, C.; Záliš, S. *J. Chem. Theor. Comput.*, submitted.
(31) Slageren, J.; Klein, A.; Záliš, S.; Stufkens D. J. *Coord. Chem. Rev.* **2001**, *219*, 937.
(32) Roos, B. O.; Andersson, K.; Fülscher, M. P.; Serrano-Andrés, L.; Siegbahn, P. E. M.; Pierloot, K.; Merchan, M.; Molina, V. *THEOCHEM* **1996**, *388*, 257.
(33) Andrae, D.; Haeussermann, U.; Dolg, M.; Stoll, H.; Preuss, H. *Theor. Chim. Acta* **1990**, *77*, 123.
(34) Bergner, A.; Dolg, M.; Kuechle, W.; Stoll, H.; Preuss, H. *Mol. Phys.* **1993**, *80*, 1431.

set contracted to [2s, 3p],[34] for the iodide atom (7 valence electrons)-a (4s, 5p) set contracted to [2s, 3p],[34] and for the H atoms a (7s) contracted to [2s].[35] The spin−orbit coupling effects which may be significant in these molecules (a few hundreds of wavenumbers) are not included in the present work and will be the subject of a further article dedicated to the photoreactivity. The ab initio calculations were carried out with the Molcas 5.0 system of programs.[36]

Vertical excitation energies and transition dipole moments have also been studied using the TD-DFT method with Ru and I atoms in the approximation of the effective core potentials described above. The cc-pVDZ (Dunning's polarized valence double-ξ) basis sets[37] were used for H, C, N, O, and Cl atoms. The influence of the size of basis sets on transition energies was examined elsewhere.[30]

In order to analyze the functional influence on the TD-DFT results, the following hybrid functionals were used: (i) the B3LYP proposed by Becke[38] that includes a mixture of Slater functional,[39] Becke's 1988 (B88) gradient correction,[40] and 23% of Hartree−Fock exchange (its correlation part, LYP, is the gradient corrected functional of Lee, Yang, and Parr),[41] and (ii) the hybrid functional of Perdew, Burke, and Ernzerhof[42] **(**PBE1PBE), which uses 25% exchange and 75% correlation weighting and BHandHLYP[38] which contains 50% of Hartree−Fock exchange. For comparison, the pure functional, BP86, which includes Slater exchange with Becke's gradient correction in conjunction with Perdew's gradient correction to local correlation functional has been used.[43] The TD-DFT calculations have been performed with the GAUSSIAN03 system of programs.[44] The solvent effects which should shift the charge-transfer transitions to the higher energies by about 0.25 eV (2000 cm^{-1}) are not taken into account in the calculations reported in the present paper.

(35) Pierloot, K.; Dumez, B.; Widmark, P.-O.; Roos, B. O. *Theor. Chim. Acta* **1995**, *90*, 87.
(36) Andersson, K.; Blomberg, M. R. A.; Fülscher, M. P.; Karlström, G.; Lindh, R.; Malmqvist, P.-Å.; Neogrady, P.; Olsen, J.; Roos, B. O.; Sadlej, A. J.; Schütz, M.; Seijo, L.; Serrano-Andrčs, L.; Sigbahn, P. E. M.; Widmark, P.-O. *Molcas 5.0*; Lund University: Sweden, 1997.
(37) Woon, D. E.; Dunning, T. H., Jr. *J. Chem. Phys.* **1993**, *98*, 1358.
(38) Becke, A. D. *J. Chem. Phys.* **1993**, *98*, 5648.
(39) Slater, J. C. *Quantum Theory of Molecules and Solids*; McGraw-Hill: New York, 1974; Vol. 4.
(40) Becke, A. D. *Phys. Rev. A* **1988**, *38*, 3098.
(41) Lee, C.; Yang, W.; Parr, R. G. *Phys. Rev. B* **1988**, *37*, 785.
(42) Perdew, J. P.; Burke, K.; Ernzerhof, M. *Phys. Rev. Lett.* **1996**, *77*, 3865; *Phys. Rev. Lett.* **1997**, *78*, 1396. Ernzerhof, M.; Scuseria, G. E. *J. Chem. Phys.* **1999**, *110*, 5029. Adamo, C.; Barone, V. *J. Chem. Phys.* **1999**, *110*, 6158.
(43) Perdew, J. P. *Phys. Rev. A* **1986**, *33*, 8822.
(44) Frisch, M. J.; Trucks, G. W.; Schlegel, H. B.; Scuseria, G. E.; Robb, M. A.; Cheeseman, J. R.; Montgomery, J. A., Jr.; Vreven, T.; Kudin, K. N.; Burant, J. C.; Millam, J. M.; Iyengar, S. S.; Tomasi, J.; Barone, V.; Mennucci, B.; Cossi, M.; Scalmani, G.; Rega, N.; Petersson, G. A.; Nakatsuji, H.; Hada, M.; Ehara, M.; Toyota, K.; Fukuda, R.; Hasegawa, J.; Ishida, M.; Nakajima, T.; Honda, Y.; Kitao, O.; Nakai, H.; Klene, M.; Li, X.; Knox, J. E.; Hratchian, H. P.; Cross, J. B.; Adamo, C.; Jaramillo, J.; Gomperts, R.; Stratmann, R. E.; Yazyev, O.; Austin, A. J.; Cammi, R.; Pomelli, C.; Ochterski, J. W.; Ayala, P. Y.; Morokuma, K.; Voth, G. A.; Salvador, P.; Dannenberg, J. J.; Zakrzewski, V. G.; Dapprich, S.; Daniels, A. D.; Strain, M. C.; Farkas, O.; Malick, D. K.; Rabuck, A. D.; Raghavachari, K.; Foresman, J. B.; Ortiz, J. V.; Cui, Q.; Baboul, A. G.; Clifford, S.; Cioslowski, J.; Stefanov, B. B.; Liu, G.; Liashenko, A.; Piskorz, P.; Komaromi, I.; Martin, R. L.; Fox, D. J.; Keith, T.; Al-Laham, M. A.; Peng, C. Y.; Nanayakkara, A.; Challacombe, M.; Gill, P. M. W.; Johnson, B.; Chen, W.; Wong, M. W.; Gonzalez, C.; Pople, J. A. *Gaussian 03*, revision A.1; Gaussian, Inc.: Pittsburgh, PA, 2003.

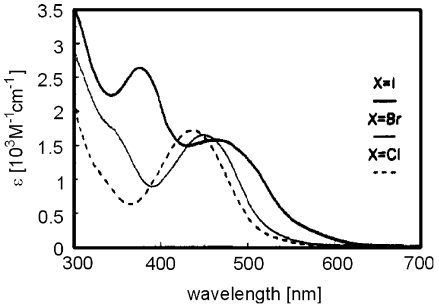

Figure 2. UV−vis absorption spectra of [Ru(X)(R) (CO)$_2$(α-diimine)] in THF solution (reproduced with the permission of the authors).[7] Reprinted with permission from ref 7. Copyright 1994 American Chemical Society.

Results and Discussion

Before reporting the theoretical interpretation of the absorption spectra of the title complexes and discussing the influence of the halide ligand on the character of the low-lying excited states of the model complexes [Ru(X)(Me)-(CO)$_2$(Me-DAB)], the experimental spectra of the ^{i}Pr-DAB complexes (X = Cl or I) will be presented.

The UV−Vis Absorption Spectra of the Complexes [Ru(Cl)(Me)(CO)$_2$(^{i}Pr-DAB)] and [Ru(I)(Me)(CO)$_2$(^{i}Pr-DAB)]. The experimental UV−vis absorption spectra of the complexes [Ru(X)(Me)(CO)$_2$(α-diimine)] are reported in Figure 2.[7]

The experimental band maxima and molar absorptivities from ref 7 (for X = Cl or I in THF) and ref 22 (for X = Cl in cyclohexane) are reported in Table 2 together with the theoretical values (vacuum). The values obtained in cyclohexane are closer to the values in a vacuum. The solvatochromism of the absorption bands of these complexes may be significant with shifts to the red of 2320 and 1870 cm^{-1}, respectively, from MeCN to toluene for the iodide complex,[7] for instance.

The two complexes have rather different absorption spectra. The spectrum of [Ru(Cl)(Me)(CO)$_2$(^{i}Pr-DAB)] exhibits one band centered at 459 nm (21 790 cm^{-1})[22] or 435 nm (22 990 cm^{-1})[7] (band I) with an unresolved shoulder at 356 nm (28 090 cm^{-1})[22] or 330 nm (30 300 cm^{-1}).[7] Band I is more intense, shifted to the red and broader with a plateau between 463 and 520 nm (21 600−19 230 cm^{-1}) when going from Cl to I. The spectrum of [Ru(I)(Me)(CO)$_2$(^{i}Pr-DAB)] differs by the presence of a second broad absorption at 374 nm (26 740 cm^{-1}). Both complexes also show an intense UV absorption starting below 300 nm (33 300 cm^{-1}). The general spectral features of the chloride complex are rather similar to the nonhalide [Ru(SnPh$_3$)$_2$(CO)$_2$(^{i}Pr-DAB)] and [Ru(Me)(SnPh$_3$)(CO)$_2$(^{i}Pr-DAB)] complexes with a single broad absorption in the visible.[22] On the basis of resonance Raman spectra,[12−15] variation of the halide from Cl to I changes the character of the lowest energy band from MLCT to XLCT which would explain the main differences in the absorption spectra of the two molecules.

Functional Influence on TD-DFT Calculated Lowest Lying Transitions. Our previous study[22] indicated that the TD-DFT systematically underestimates transition energies of halide complexes, although the general spectral pattern

Table 1. TD-DFT Transition Energies (in cm^{-1}) to the Low-Lying $^1A'$ States (with Nonzero Oscillator Strengths) of [Ru(Me)(X)$(CO)_2$(Me-DAB)] (X = Cl, SnH_3, I) Complexes Calculated with Different BP86, B3LYP, PBE1PBE, and BHandHLYP Functionals (Oscillator Strengths in Parentheses)

transition	BP86	B3LYP	PBE1PBE	BHandHLYP	experiment
		X = Cl			
XLCT/MLCT $a^1A' \rightarrow b^1A'$	12 090 (0.006)	16 210 (0.011)	17 640 (0.013)	24 440 (0.021)	21 790[a]
SBLCT $a^1A' \rightarrow c^1A'$	20 240 (0.006)	23 310 (0.015)	24 780 (0.018)	29 840 (0.028)	28 090[a]
MLCT/XLCT $a^1A' \rightarrow e^1A'$	24 560 (0.067)	27 500 (0.060)	28 840 (0.057)	35 890 (0.032)	
		X = I			
XLCT $a^1A' \rightarrow b^1A'$	10 329 (0.002)	13 912 (0.003)	15 070 (0.004)	20 618 (0.005)	21 600[b]
SBLCT $a^1A' \rightarrow c^1A'$	19 837 (0.023)	22 284 (0.044)	23 450 (0.052)	27 052 (0.076)	26 737[b]
MLCT $d^1A' \rightarrow d^1A'$	23 861 (0.043)	26 474 (0.059)	27 510 (0.055)	32 868 (0.035)	>33 300[b]
		X = SnH_3			
SBLCT $a^1A' \rightarrow b^1A'$	19 870 (0.034)	22 020 (0.063)	22 260 (0.069)	23 560 (0.106)	18 900[a]
MLCT $a^1A' \rightarrow e^1A'$	25 790 (0.072)	29 760 (0.042)	28 080 (0.058)	31 440 (0.039)	32 260[a]

[a] Experimental band maxima from ref 22 (in cyclohexane). [b] Experimental band maxima from ref 7 (in THF).

Table 2. Lowest Part of the Near-UV−Vis Absorption Spectra of [Ru(Me)(Cl)$(CO)_2$(Me-DAB)] and [Ru(Me)(I)$(CO)_2$(Me-DAB)][a]

experiment[b]	transition	CASSCF/CASPT2	TD-DFT[c]
	X = Cl		
22 990 (21 790)	$a^1A' \rightarrow b^1A'$	18 890 (0.08)	17 640 (0.013)
435 nm, 1710 (459 nm, 1760)		MLCT/XLCT	XLCT/MLCT
30 300 (28 090)	$a^1A' \rightarrow c^1A'$	26 520 (0.08)	24 780 (0.018)
~330 nm, ~1100 (356 nm, 1240)		SBLCT	SBLCT
	$a^1A' \rightarrow d^1A'$	28 780 (0.0)	28 410 (0.0)
		MLCT	MLCT
	$a^1A' \rightarrow e^1A'$	30 200 (0.10)	28 840 (0.057)
		XLCT/MLCT	MLCT/XLCT
	X = I		
21 600	$a^1A' \rightarrow b^1A'$	18 690 (0.03)	15 070 (0.004)
463 nm, 1555		XLCT	XLCT
26 737	$a^1A' \rightarrow c^1A'$	24 810 (0.22)	23 450 (0.052)
374 nm, 2630		SBLCT	SBLCT
(>33 300)	$a^1A' \rightarrow d^1A'$	29 330 (0.16)	27 510 (0.055)
		MLCT	MLCT

[a] Transition energies in cm^{-1}, oscillator strengths in parenthesis. [b] Experimental band maxima and molar absorptivities (M^{-1} cm^{-1}) from ref 7 in THF and ref 22 in cyclohexane (in parentheses). [c] PBE1PBE hybrid functional.

is well reproduced. A similar problem was recently put in evidence in the halide containing system $CuCl_4^-$.[28] Table 1 summarizes the lowest calculated transition energies and oscillator strengths obtained at the TD-DFT level with various functionals for [Ru(Cl)(Me)$(CO)_2$(Me-DAB)], [Ru(I)(Me)$(CO)_2$(Me-DAB)], and, for comparison, [Ru(SnH_3)(Me)$(CO)_2$(Me-DAB)].

The lowest allowed electronic transition $a^1A' \rightarrow b^1A'$ of the chloride complex is described as originating predominantly in $3p_{Cl}/4d_{xz} \rightarrow \pi^*_{DAB}$ excitation. This electronic transition corresponds to a mixed XLCT/MLCT state with a predominant XLCT character, in contrast to the MLCT assignment obtained at the CASSCF/CASPT2 level. The assignment of the weak UV band of [Ru(Cl)(Me)$(CO)_2$(^{i}Pr-DAB)] to a SBLCT (σ-bond-to-ligand charge-transfer: $\sigma \rightarrow \pi^*$) transition agrees in both methods. The choice of the functional has a dramatic influence on the transition energies to the predominantly XLCT states in [Ru(Cl)(Me)$(CO)_2$(Me-DAB)] and [Ru(I)(Me)$(CO)_2$(Me-DAB)] as illustrated in Table 1; the use of pure BP86 functional leads to a lowering of the excited states by more than 4000 cm^{-1}. The hybrid PBE1PBE functional improves the transition energies but has no effect on the electronic character of the low-lying b^1A' and c^1A' states, still assigned to XLCT/MLCT and SBLCT, respectively. Contrary to the dramatic functional dependence of the calculated transition energies of two halide complexes, only a moderate effect is seen for [Ru(SnH_3)(Me)$(CO)_2$(Me-DAB)] (Table 1).

The basis set effect as well as the use of effective core pseudopotentials on all atoms have nearly no effect on the calculated transition energies as explained in our paper devoted to the computational aspects of the present work.[30]

In order to illustrate the effect of the contribution of HF exchange in a hybrid functional, a calculation was performed with the following hybrid BLYP functional (*a* is a parameter varying from 0 to 1) (see also the work published recently on $CuCl_4^-$, ref 28):

$$E_{xc} = a^*E_x^{HF} + (1 - a)(E_x^{LSDA} + \Delta E^{B88}) + E_c^{LYP}$$

Figure 3 reports the transition energies to the low lying $^1A'$ states of [Ru(Me)(X)$(CO)_2$(Me-DAB)] (X = Cl, SnH_3) as a function of the HF exchange percentage. The contribution of HF exchange up to 50% (common in standard hybrid functionals) influences slightly the transition energies calculated for [Ru(SnH_3)(Me)$(CO)_2$(Me-DAB)], the effect being more pronounced for the MLCT state. In contrast the transition energy calculated for the [Ru(Cl)(Me)$(CO)_2$(Me-DAB)] complex by the BHandHLYP functional (50% of HF exchange) is two times larger than that obtained using the pure LYP functional. The results reported in Table 1 and Figure 3 show that both XLCT/MLCT and SBLCT transition energies sharply increase with increasing contribution of HF exchange. It is striking that the varying functional composition shifts the calculated transition energies of [Ru(Me)(X)$(CO)_2$(Me-DAB)] across the whole visible and near-UV spectral region. Compared with the experimental values, pure functionals strongly underestimate the transition energies. On the other hand, they are overestimated with functionals containing more than 50% of HF exchange. The best agreement with experiment is obtained with the hybrid PBE1PBE functional (25% of HF exchange). This functional is used in further calculations discussed in the next section.

CASSCF/CASPT2 and TD-DFT Interpretation of Near-UV−Vis Absorption Spectra of [Ru(X)(Me)$(CO)_2$(^{i}Pr-DAB)] (X = Cl, I), Approximated by Model Systems [Ru(X)(Me)$(CO)_2$(Me-DAB)]. The CASSCF/CASPT2 and

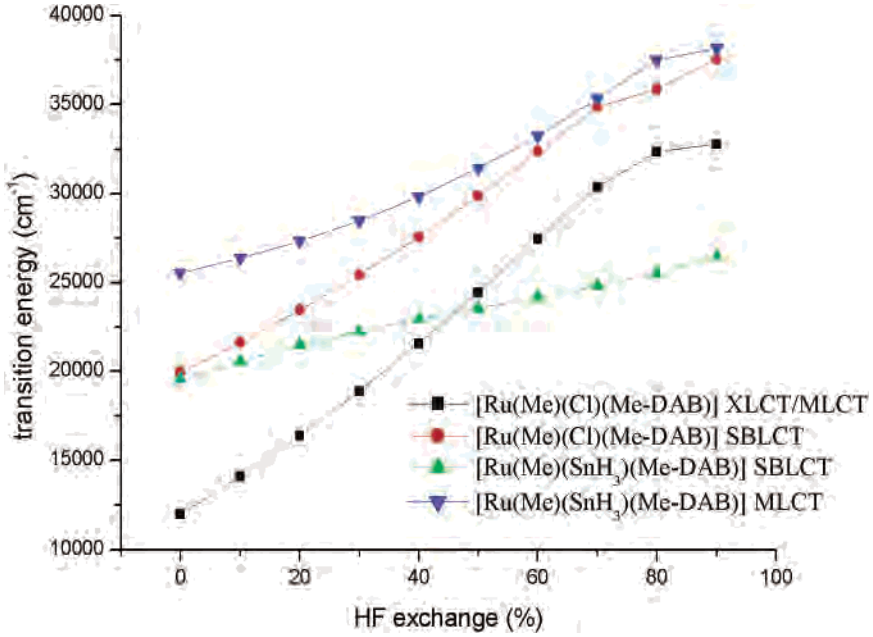

Figure 3. Dependence of the low-lying ^{1}A′ states of [Ru(Me)(X)(CO)$_2$(Me-DAB)] (X = Cl, SnH$_3$) on the amount of HF exchange.

TD-DFT transition energies to the low-lying singlet A′ states of [Ru(Cl)(Me)(CO)$_2$(Me-DAB)] are reported in Table 2together with the positions of the experimental bands for comparison. The experimental spectra are reported either in THF[7] or in cyclohexane[22] while the calculations are performed in a vacuum. In our analysis, we have to consider that the solvent correction to the charge transfer states would shift them to higher energies by about 2000−3000 cm^{-1}. The transitions to singlet A″ states are not reported here since they do not differ in both complexes (X = Cl or I) and are characterized by weak oscillator strengths.[22,30]

The MLCT/XLCT transition of mixed character (56% MLCT/19% XLCT at the CASSCF level) calculated at 18 890 cm^{-1} by CASSCF/CASPT2 has been identified as the main contributor to the lowest band of [Ru(Cl)(Me)(CO)$_2$-(Me-DAB)] observed at 22 990 cm^{-1} [7] (21 790 cm^{-1} in cyclohexane).[22] This band is assigned to a XLCT/MLCT transition calculated at 17 640 cm^{-1} at the TD-DFT level.

The small shoulder observed at 28 090 cm^{-1} (356 nm in cyclohexane)[22] or 30 300 cm^{-1} (330 nm in THF)[7] is composed mainly of two transitions with significant oscillator strengths: (i) the c^{1}A′ SBLCT ($\sigma_{\mathrm{MeRuCl}} \rightarrow \pi^*_{\mathrm{Me-DAB}}$) calculated at 26 520 cm^{-1} by CASPT2 and 24 780 cm^{-1} by TD-DFT; (ii) the XLCT/MLCT e^{1}A′ state calculated at 30 200 cm^{-1} or 28 840 cm^{-1} (TD-DFT). This CASPT2 assignment should be more likely than the one suggested by the TD-DFT results, namely a mixed state of MLCT predominant character calculated at 28 840 cm^{-1} corresponding to an intense band not observed in this domain of energy.

As pointed out in the previous section, these results illustrate the difficulty in describing correctly the excited states of mixed character and the dramatic effect of the quality of the zero-order wave function on the transition energies. The MLCT/XLCT mixed character is established by the accurate CASSCF/CASPT2 calculations; the XLCT component is probably overestimated by the means of the TD-DFT approach. Nevertheless, the lowest band which characterizes the spectrum of [Ru(Cl)(Me)(CO)$_2$(^{i}Pr-DAB)] is due to a transition to a state which remains mainly MLCT in character in agreement with the UV−vis and resonance Raman experiments.

A comparison between the CASSCF/MS-CASPT2 and TD-DFT transition energies to the low-lying singlet A′ states of [Ru(I)(Me)(CO)$_2$(Me-DAB)] reported in Table 2 indicates that both methods agree as far as the assignment of the vis−near-UV absorption spectrum of this molecule is concerned. The lowest band observed at 21 600 cm^{-1} can be assigned to a nearly pure b^{1}A′ XLCT state (>75% XLCT at the CASSCF level) corresponding to a charge transfer from I to the Me-DAB group. This state is calculated at 18 690 cm^{-1} while TD-DFT transition energy is underestimated at 15 070 cm^{-1}. The next state corresponding to the c^{1}A′ SBLCT contributes to the second band detected at 26 737 cm^{-1} and calculated at 24 810 cm^{-1} (23 450 cm^{-1} at the TD-DFT level). The presence of an MLCT state calculated at 29 330 cm^{-1} explains the occurrence of an intense band starting beyond 33 300 cm^{-1} in THF (Figure 2).

Comparison between the Absorption Spectra of [Ru(Cl)(Me)(CO)$_2$(Me-DAB)] and [Ru(I)(Me)(CO)$_2$(Me-DAB)]. The calculated transition energies to the low-lying singlet excited states of the model systems [Ru(X)(Me)(CO)$_2$(Me-DAB)] (X = Cl, I) are reported in Table 2, together with the experimental absorption maxima of the real ^{i}Pr-DAB molecules are compared.

In contrast to the chloride complex, the iodide complex is characterized by an XLCT low-lying excited state corresponding to a 5p (I) $\rightarrow \pi^*_{\mathrm{DAB}}$ excitation in agreement with the resonance Raman data.[7−9] This state calculated at 18 690 cm^{-1} (15 070 cm^{-1} at the TD-DFT level) is characterized by a low oscillator strength and should contribute to the first absorption at 463 nm. Both TD-DFT and CASSCF/MS-CASPT2 indicate nearly pure XLCT character. The next

Table 3. Changes in Mulliken Population Accompanying the Lowest Allowed Transitions within [Ru(Me)(Cl)$(CO)_2$(Me-DAB)] and [Ru(Me)(I)$(CO)_2$(Me-DAB)] According to the Different Methods (CASPT2 and TD-DFT)

method	Ru	Me	X	$(CO)_2$	Me-DAB	character of the transition
			Cl, b1A′			
CASPT2	−0.109	−0.089	−0.302	−0.061	0.561	MLCT/XLCT
TD DFT[a]	−0.190	−0.006	−0.587	−0.005	0.789	XLCT/MLCT
TD DFT[b]	−0.163	−0.005	−0.612	−0.006	0.786	XLCT/MLCT
TD DFT[c]	−0.073	0.003	−0.680	0.005	0.746	XLCT/MLCT
			Cl, c^1A'			
CASPT2	−0.077	−0.232	−0.247	−0.018	0.574	SBLCT
TD DFT[a]	−0.067	−0.368	−0.336	−0.023	0.794	SBLCT
TD DFT[b]	−0.060	−0.353	−0.346	−0.032	0.792	SBLCT
TD DFT[c]	−0.062	−0.317	−0.354	−0.041	0.774	SBLCT
			I, b^1A'			
CASPT2	−0.138	−0.079	−0.375	0.050	0.541	XLCT/MLCT
TD DFT[a]	−0.035	0.004	−0.761	0.018	0.774	XLCT
			I, c^1A'			
CASPT2	−0.142	−0.130	−0.176	0.021	0.427	SBLCT
TD DFT[a]	−0.044	−0.240	−0.403	−0.025	0.713	SBLCT
			I, d^1A'			
CASPT2	−0.234	−0.050	−0.106	−0.084	0.474	MLCT
TD DFT[a]	−0.526	−0.049	−0.043	−0.065	0.684	MLCT

[a] With the hybrid PBE1PBE functional. [b] With the functional B3LYP. [c] With the functional BP86.

higher state corresponds to an SBLCT transition calculated at 24 810 cm^{-1} (23 450 cm^{-1} with TD-DFT) which should contribute to the absorption maximum detected at 374 nm (26 737 cm^{-1}). The MLCT ($4d_{xz} \rightarrow \pi^*_{DAB}$) state which characterizes the lowest part of the spectrum of the chloride complex is shifted to the higher energies at 29 330 cm^{-1} (27 510 cm^{-1} with TD-DFT) and is responsible for the broad absorption starting below 300 nm (33 300 cm^{-1}).

The calculated changes in Mulliken populations during the lowest allowed transitions in the model complexes (Table 3) illustrate perfectly the differences of characters of the low-lying excited states in both molecules. Moreover, this table gives a comparison of these changes as a function of the computational method. The charge redistribution in the course of the lowest excitation within [Ru(Cl)(Me)$(CO)_2$-(Me-DAB)] indicates the mixed MLCT/XLCT character with prevailing XLCT component in the case of DFT calculations. The TD-DFT results obtained with hybrid functionals are closer to CASPT2 results; nevertheless, there is the larger overall charge separation than CASPT2 shows. This table also confirms the larger XLCT character of the lowest lying b^1A' state in the case of X = I, with DFT predicting the greater increasing of X contribution going from Cl to I.

Conclusion

A detailed analysis of the UV−vis absorption spectra of [Ru(X)(Me)$(CO)_2$(Me-DAB)] (X = Cl, I) complexes, based on ab initio and TD-DFT calculations, has enabled a quantitative assignment of the lowest bands. In agreement with time-resolved emission, IR, and stationary resonance Raman experiments, the lowest excited state changes from MLCT to XLCT character on going from the chloride to the iodide complex. The next higher state in both complexes corresponds to an SBLCT transition whereas the near-UV spectrum starts with a predominantly XLCT band in [Ru-(Cl)(Me)$(CO)_2$(Me-DAB)] and an MLCT band in [Ru(I)-(Me)$(CO)_2$(Me-DAB)]. This remarkable difference in the absorption spectrum may have significant consequences on the photophysics and photochemistry of this class of molecules. As stressed out in our theoretical paper,[30] calculated transitions energies are appreciably affected by the choice of the computational strategy (CASSCF active space, number of averaged roots). The TD-DFT assignment differs significantly from the ab initio one pointing to a predominant XLCT character of the lowest singlet state even for the chloro complex. The influence of the functional on the transition energies of [Ru(X)(Me)$(CO)_2$(Me-DAB)] is dramatic as well. The transition energies calculated by the TD-DFT method with pure functionals are strongly underestimated; the inclusion of HF exchange provides the transition energies closer to experimental values. This effect seems to be due to the presence of a halide ligand, the interaction of which with the metal center being poorly described by the DFT method. This hypothesis is corroborated by the fact that the TD-DFT transition energies to the low-lying SBLCT and MLCT states of the nonhalide complex [Ru(SnH_3)(Me)$(CO)_2$(Me-DAB)] are well described and depend on the functional only moderately. Moreover, if the ab initio calculations put in evidence an increasing $4d_{Ru}$/*n*p(X) metal−halide interaction on going from the chloride to the iodide, the variation of this interaction in [Ru(Cl)-(Me)$(CO)_2$(Me-DAB)] and [Ru(I)(Me)$(CO)_2$(Me-DAB)] is only moderate in the case of Kohn−Sham orbitals. Both methods reproduce well the red shift of the lowest absorption band and the shift of the strong MLCT band from the visible to the near-UV domain of energy when the Cl ligand is replaced by I. In the present study, the solvent effects are not taken into account. Solvent corrections may perturb significantly the calculated spectra but should not modify the qualitative conclusions and assignment.

As far as the photoreactivity is concerned, preliminary simulations of wave packet dynamics have been performed on the 1-D potential energy curves calculated for the Ru−Me homolysis in [Ru(Cl)(Me)$(CO)_2$(Me-DAB)].[45] In these simulations, the MLCT/XLCT absorbing state has been coupled by spin−orbit (SO) to the low-lying predissociative b^3MLCT (SOC = 180 cm^{-1}) and emissive a^3MLCT states (SOC = 375 cm^{-1}). The main conclusion is that the photoreactivity is not only controlled by the barrier hight generated by the avoided crossing between the b^3MLCT and ^{3}SBLCT states but also controlled by the SO. In the model complex, the a^3MLCT emissive state is preferably populated, confirming the photostability of the chloride complex. The SO effects should be even more pronounced for the iodide complex. A further study should be devoted to the photodissociation dynamics of [Ru(I)(Me)$(CO)_2$(Me-DAB)] before concluding about the photoreactivity of this class of halides complexes.

Acknowledgment. This work has been undertaken as a part of the European collaborative COST project (D14/0001/

(45) Turki, M.; Daniel, C. To be submitted.

99). We thank the Departement de Chimie of the CNRS and the Ministry of Education of the Czech Republic (OC.D14.20) for specific COST financial support. The authors are grateful to Prof. A. Vlček, Jr., and Dr. M. Bénard for stimulating discussions. The calculations have been carried out in part at the Centre Universitaire et Régional de Ressources Informatiques (CURRI, Université Louis Pasteur, Strasbourg, France), in part at the IDRIS computer center (CNRS, Orsay, France) through a grant of computer time from the Conseil Scientifique, at the LCQS (Strasbourg, France), and at the computer facilities at the J. Heyrovský Institute of Physical Chemistry.

IC049464E